NJC

PAPER

View Article Online
View Journal | View Issue

Cite this: *New J. Chem.*, 2018, **42**, 15770

A peptide-based multifunctional fluorescent probe for Cu^{2+}, Hg^{2+} and biothiols†

Xuliang Pang,[a] Lei Gao,‡[b] Huiyun Feng,[a] Xudong Li,[b] Jinming Kong[c] and Lianzhi Li*[a]

A peptide-based fluorescent probe (Dansyl-His-Pro-Gly-Trp-NH_2, D-P4) bearing the dansyl fluorophore and tryptophan residue has been developed for the detection of Hg^{2+}, Cu^{2+} and biothiols (–SH). DP-4 exhibited high selectivity and sensitivity for Cu^{2+} and Hg^{2+} in the presence of 17 metal ions and 6 anions. D-P4 could differentiate Hg^{2+} and Cu^{2+} *via* a ratiometric response toward Hg^{2+} and quenching response toward Cu^{2+}. Upon the addition of Hg^{2+} or Cu^{2+} ions, the D-P4 solution displayed a colour change, which was visible to the naked eyes under a UV lamp. The limits of detection (LOD) of DP-4 are 37 nM for Hg^{2+} and 105 nM for Cu^{2+}, which for Cu^{2+} is much lower than the EPA drinking water maximum contaminant level. Additionally, the binding stoichiometry, binding affinity and pH influence of D-P4 for Hg^{2+} and Cu^{2+} ions were studied. Determination of Hg^{2+} and Cu^{2+} in river water samples with D-P4 showed satisfactory results. It is noteworthy that the D-P4-Hg system could be regenerated using cysteine (Cys), which was confirmed *via* circular dichroism (CD) and UV-vis absorption spectroscopy. Moreover, the D-P4-Hg system could be used to detect cysteine, homocysteine (Hcy) and glutathione (GSH). These results indicate that the D-P4-Hg system can selectively detect cysteine among the 20 common amino acids with an LOD of 82 nM.

Received 20th July 2018,
Accepted 21st August 2018

DOI: 10.1039/c8nj03624a

rsc.li/njc

Introduction

Heavy and transition metal (HTM) ions are non-biodegradable contaminants in living organisms, which represent a growing environmental problem and have affected various components of the environment, including the terrestrial and aquatic biota.[1] Some heavy metals, including mercury (Hg), lead (Pb), arsenic (As), cadmium (Cd) and chromium (Cr), are highly toxic and hazardous to living organisms.[2,3] Among the various HTM ions, Hg^{2+} is considered to be the most toxic and hazardous to humans and biological organisms, which is released by many anthropogenic sources such as coal plants, oil drilling, steel plants, mercury lamps, barometers and thermometers.[4,5] In general, inorganic or organic mercury enters from the surroundings to the food chain through contaminated water or polluted air and accumulates in higher organisms, which can further cause several severe diseases, including Hunter-Russell syndrome, acrodynia, anaemia, dermatitis, gastric disorders and Minamata disease.[6–9] As the third most abundant transition metal ion in living organisms, Cu^{2+} also plays a key role in various biological processes, and its homeostasis is critical for the metabolism and development of humans and biological organisms.[10–12] HTM ions are released into the environment through cosmetics and their by-products, fertilizers and other chemicals generated from industrial wastewater and household waste. According to the United States Environmental Protection Agency (USEPA), the permissible drinking water maximum contaminant levels of Hg^{2+} and Cu^{2+} are 2 ppb (10 nM) and 1.3 ppm (20 μM), respectively.[13,14] Therefore, it is of great importance to establish fast, accurate and reliable techniques for the detection of HTM ions. Table 1 lists some recent reports on spectrofluorimetric and spectrophotometric sensing systems for the determination of Cu^{2+} and Hg^{2+}.[15–34] Among them, peptide-based probes have received considerable attention due to their easy synthesis, timely response and biocompatibility.[35–37] The selectivity of peptide-based probes mainly depends on the metal chelating ability of the amino acid residues in their receptors.[38] According to the analysis of the Protein Data Bank (PDB), some special amino acid residues are easily chelated to metal ions in biological systems, such as the carboxyl groups of glutamic acid (Glu) and aspartic acid (Asp), imidazole groups of histidine (His) and sulfhydryl groups of cysteine (Cys).[39] The imidazole group of histidine and the indole group of tryptophan can be used as active ligands in the chelation of

[a] *School of Chemistry and Chemical Engineering, Liaocheng University, Liaocheng 252059, P. R. China. E-mail: lilianzhi1963@163.com*
[b] *Liaocheng People's Hospital, Liaocheng 252000, P. R. China*
[c] *School of Environmental and Biological Engineering, Nanjing University of Science and Technology, 200 Xiaolingwei, Nanjing 210094, China*

† Electronic supplementary information (ESI) available: Additional figures. See DOI: 10.1039/c8nj03624a

‡ Co-first author.

Table 1 (a) Various spectroscopic sensing systems for the determination of Cu^{2+}. (b) Various spectroscopic sensing systems for the determination of Hg^{2+}

Method	System	Detection limit	Ref.
(a)			
Fluorescence	Dansyl-MH	95.0 nM	15
Fluorescence	Dansyl-HKH-Dansyl	78.0 nM	16
Fluorescence	Dansyl-GGDGGDGGDGGDGGW	500.0 nM	17
Fluorescence	Dansyl-HPGW	105.0 nM	This study
Fluorescence	DNAzyme	35.0 nM	18
Fluorescence	Cyclam derivative	260.0 nM	19
Fluorescence	2-Hydroxy-1-naphthaldehyde based ADA	15.8 nM	20
Fluorescence	BODIPY	200.0 nM	21
Absorption	1,5-naphthalenediamine based Schiff base	19.0 nM	22
Absorption	Naphthalimide-based Schiff base	10.0 μM	23
Absorption	*N*-Butylbenzene-1,2-diamine	3.97 μM	24
(b)			
Fluorescence	Unnatural amino acids conjugated with dansyl	9.3 nM	25
Fluorescence	Dansyl-P23	1.4 μM	26
Fluorescence	Dansyl-AACAAHCWAE	25.9 nM	27
Fluorescence	NBD-CC-NBD	25.6 nM	28
Fluorescence	Dansyl-HPGW	37.0 nM	This study
Fluorescence	Pyr-Y	12.0 nM	29
Fluorescence	Rhodamine B derivative	50 nM	30
Fluorescence	Cyclam derivative	7.9 μM	19
Fluorescence	A new rhodamine derivative	120.0 nM	32
Fluorescence	*N*-[*p*-(Dimethylamino)benzamido]-*N*′-phenylthiourea	39.0 nM	33
Absorption	DNA-functionalized gold nanoparticles	60.0 nM	34
Absorption	Schiff-based colorimetric chemosensor	390.0 nM	9

metal ions.[40,41] Although some amino acids or peptide-based probes have been developed for metal ion monitoring, multi-analyte recognition using a unique class of sensors remains a major challenge.[22] Only a few examples of fluorescence sensors show a ratiometric response to Hg^{2+} and can regenerate their ability for detection using cysteine.[42,43] Intracellular thiols, including Cys, Hcy and GSH, play vital roles in cellular function and metabolism.[44] For example, protein thiol groups are crucial for the formation of the mitotic apparatus.[45] Cys, as one of the basic amino acids, is involved in the formation of the three-dimensional structure of protein.[46] Several studies have indicated that Cys can balance the concentration of heavy metal ions in biological processes. Moreover, Cys is essential for the activity of many proteins, where protein disorders are closely related to Alzheimer's and Parkinson's diseases.[47,48] Moreover, Hcy is structurally similar to Cys, but its functions *in vivo* are entirely different. Hcy level is considered as one of the important parameters for cardiovascular disease and Alzheimer's disease.[49] GSH is a very important tripeptide in the human body, and a change in the cellular GSH level is associated with several diseases, such as leucocyte loss, HIV infection and liver damage.[46] Thus, the detection of biothiols is of great significance.

Herein, a new peptide-based fluorescent probe (Dansyl-His-Pro-Gly-Trp-NH_2, DP-4) was synthesized, and could monitor Cu^{2+} *via* a turn-off response and Hg^{2+} *via* a ratiometric response with very low LODs in 10 mM HEPES buffer solution. Moreover, the D-P4-Hg system showed an exclusive response to biothiols (Cys, Hcy, and GSH). Scheme 1 displays the possible binding modes of D-P4 with Cu^{2+}, Hg^{2+} and biothiols. Importantly, this study provides the new possibility of using a simple peptide-based probe for multidetection. We also expect that this probe could have practical applications in the environmental and biological fields.

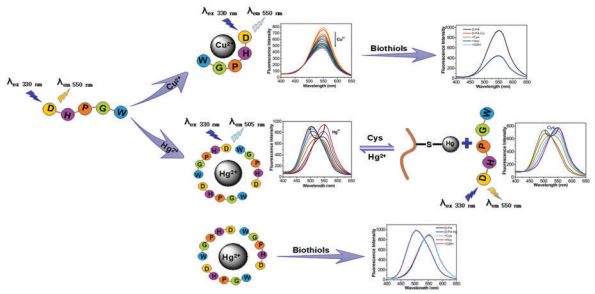

Scheme 1 Proposed binding modes of D-P4 with Cu^{2+}, Hg^{2+} and biothiols.

Experimental

Materials and instruments

Fmoc–His(Trt)–OH, Fmoc-Pro-OH, Fmoc-Gly-OH, Fmoc-Trp(Boc)-OH and Rink Amide resin were purchased from CSBio. Co., USA. Trifluoroacetic acid (TFA) and dansyl chloride were purchased from Shanghai Macklin Biochemical Co., Ltd. Tri-isopropylsilane (TIS), *N*,*N*′-diisopropylcarbodiimide (DIC), 2-(1*H*-benzotriazole-1-yl)-1,1,3,3-tetramethyluronium hexafluorophosphate (HBTU) and *N*,*N*-diisopropylethylamine (DIEA) were purchased from Shanghai GL Biochem Ltd. Amino acids, homocysteine (Hcy) and glutathione (GSH) were purchased from Sigma Chemical Co. Ltd. Other chemical reagents were analytical grade unless otherwise noted. All metal ion salt sample solutions were prepared in 10 mM HEPES buffer solution at pH 7.1.

Instruments included CS 136 Peptide Synthesizer (CS Bio Co., USA), API 4500 QTRAP Mass Spectrometer (Applied Biosystems/MDS SCIEX, USA), High Performance Liquid Chromatography (HPLC) system (model 426 HPLC pump, UVIS 201 detector, Alltech, USA), Hitachi F-7000 fluorescence spectrofluorometer (Hitachi Inc., Japan), Jasco J-810 circular dichroism (CD) spectrophotometer (Japan) and Lambda 750 UV-visible absorption spectrophotometer (Perkin Elmer, USA).

Solid phase synthesis of D-P4

Dansyl-His-Pro-Gly-Trp-NH_2 (D-P4) was synthesized using Fmoc chemistry and solid phase peptide synthesis technology. Fmoc-protected Fmoc-Trp(Boc)-OH (0.6 mmol) was assembled on Rink Amide resin (0.2 mmol). After deprotecting the Fmoc group from the resin-bound Trp, Fmoc-Gly-OH (0.6 mmol), Fmoc-Pro-OH (0.6 mmol) and Fmoc-His(Trt)-OH (0.6 mmol) were assembled, successively. Then, dansyl chloride (0.6 mmol) in DMF was added to the resin bound tetrapeptide. Cleavage of the peptide from the resin was achieved *via* treatment with a mixture of 6.0 mL TFA : thioanisole : phenol : H_2O : EDT (82.5 : 5 : 5 : 5 : 2.5, v/v/v/v/v) in a dark room at room temperature for 3 h. The crude DP-4 was precipitated in ice-cold ether and then centrifuged at 8000 rpm for 10 min at −4 °C. The crude peptide was purified *via* high-performance liquid chromatography (HPLC) using a C18 column. Mobile phase A was 0.1% TFA solution and mobile phase B was methanol. ESI mass spectrometry was performed in positive ion mode with the following operating parameters: the electrospray voltage, 5500 V; curtain gas, 20 psi; GS 1, 45 psi; and GS 2, 50 psi. The source temperature was 500 °C, and nitrogen was used as the nebulizer and desolvation gas.

Fluorescence spectra measurement

Initially, 3.0 mM D-P4 stock solution was prepared in 10 mM HEPES buffer (pH = 7.1) and stored in a dark room at 4 °C. The stock solution of D-P4 was appropriately diluted for all spectral measurements. Each metal ion and anion solution was prepared in 10 mM HEPES buffer (pH 7.1). The fluorescence spectra (350–650 nm) of D-P4 in the absence and presence of 17 metal ions (Cr^{3+}, Mn^{2+}, Fe^{3+}, Co^{2+}, Ni^{2+}, Zn^{2+}, Cd^{2+}, Hg^{2+}, Pb^{2+}, Al^{3+}, Ca^{2+}, Mg^{2+}, K^+ and Na^+ as chloride salts, Fe^{2+} and Cu^{2+} as sulfate salts, and Ag^+ as nitrate salt) and 6 anions ($NaNO_3$, Na_2SO_4, Na_3PO_4, $NaClO_4$, NaAc and NaCl) were measured with excitation of 295 nm and 330 nm in 10 mM HEPES buffer (pH 7.1), respectively. The fluorescence spectra of D-P4-Hg in the presence of 20 amino acids, Hcy and GSH were also measured under the same conditions. Both excitation and emission wavelength slit widths were 5 nm.

pH influence on fluorescence spectra

Fluorescence emission spectra of the D-P4, D-P4-Cu^{2+} and D-P4-Hg^{2+} systems were measured at different pH with excitation of 330 nm. The pH value of the sample solution was adjusted by appropriate additions of $HClO_4$ or NaOH solutions.

Binding stoichiometry and binding constant

The binding stoichiometry of this probe was obtained from the Job's plot between the mole fraction of Cu^{2+} and Hg^{2+} and relative emission intensity. The binding constant was obtained from the modified Benesi–Hildebrand equation:[50,51] $\Delta FI_{max}/\Delta FI = 1 + ([M]^{-n}/K)$, where ΔFI_{max} is $FI_{max} - FI_0$, ΔFI is $F_x - F_0$, F_0 is the emission intensity of D-P4, F_x is the emission intensity of D-P4 in the presence of a relative concentration of Hg^{2+} and Cu^{2+}, [M] is the concentration of Hg^{2+} and Cu^{2+}, and K is the binding constant.

Limit of detection

The limit of detection (LOD) was calculated using the data from the fluorescence titration experiments as follows: LOD = $3\sigma/m$, where σ is the standard deviation of the blank measurement, which was obtained from the fluorescence intensity of D-P4 in the absence of Cu^{2+} or Hg^{2+} and measured ten times, m is the slope of the fluorescence intensity *versus* the concentration of Cu^{2+} or Hg^{2+} ion. The detection limit of cysteine for the D-P4-Hg system was also calculated using this equation.[52]

Application for the detection of Cu^{2+} and Hg^{2+} in river water

To test the practical application of the D-P4 probe, it was applied for the determination of Cu^{2+} and Hg^{2+} in river water samples. The measured river water samples were simply filtered previously to remove impurities. The pH of the river water was adjusted to 7.1. The level of Hg^{2+} in the river samples was determined using the standard addition method. The fluorescence spectra of D-P4 in the presence of a series of low concentrations of Cu^{2+} or Hg^{2+} ions in river water at pH 7.1 were measured.

UV/Vis and CD spectra studies

The UV-vis absorption spectra of D-P4 in the presence of Cu^{2+} and Hg^{2+} ions were measured in 10 mM HEPES solution at pH 7.1. CD spectra were recorded on a Jasco J-810 spectropolarimeter in the range of 250–190 nm with 1 cm path length quartz optical cell at room temperature. Each spectrum was the average of three accumulations at a 1 s-response time with a data pitch of 0.5 nm and scan speed of 200 nm min^{-1}.

Results and discussion

Solid phase peptide synthesis

The fluorescent peptide probe (Dansyl-His-Pro-Gly-Trp-NH_2, D-P4) was synthesized *via* solid phase peptide synthesis technology. After cleavage of the product from Rink Amide resin, D-P4 was purified from the crude product by HPLC with a C18 column. The successful synthesis was confirmed by ESI mass spectrometry. ESI mass of DP-4 calculated: 728.83 [M + H^+]; observed: 728.3 [M + H^+]. DP-4 exhibits good solubility in 100% aqueous solution.

Fluorescence response of D-P4 with metal ions and anions

Fig. 1a shows the fluorescence response of the probe to 17 metal ions and 6 anions with the excitation wavelength of 330 nm in 10 mM HEPES solution at pH 7.1. The results indicated that D-P4 displays excellent sensitivity and high selectivity for Cu^{2+} and Hg^{2+} ions among the tested ions, and there was no response for the other various metal ions and anions.

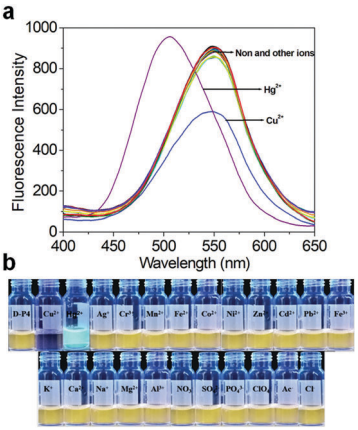

Fig. 1 (a) Fluorescence spectra of DP-4 (20 μM) excited at 330 nm in the presence of various ions in 10 mM HEPES buffer at pH 7.1. The molar ratio of metal/D-P4 was 1 : 1. (b) Emission color changes of the systems excited by a UV lamp (365 nm).

Fig. 1b presents the color changes of the D-P4 solution in the absence and presence of Cu^{2+}, Hg^{2+} and other ions excited by a 365 nm UV lamp. The D-P4 solution itself was yellow in color. The addition of Cu^{2+} to the D-P4 solution caused its color to change from yellow to colorless, and Hg^{2+} changed the D-P4 solution color from yellow to green. However, the D-P4 solutions containing the other 15 metal ions retained their yellow color.

To investigate the interference effect of 16 other metal ions and 6 anions on the detection ability of DP-4 for Cu^{2+} and Hg^{2+}, the fluorescence responses of DP-4 to Cu^{2+} and Hg^{2+} were measured in the presence of these ions. Fig. 2 shows the fluorescence responses of this probe in the absence and presence of different ions systems. The results indicate that the fluorescence response of DP-4 for Cu^{2+} is not affected by the 15 metal ions and 6 anions except Hg^{2+}, and we still could differentiate Hg^{2+} because it caused a blue shift in the fluorescence from 550 nm to 505 nm (Fig. 1a). Moreover, the detection of Hg^{2+} was not interfered by all the ions including Cu^{2+}.

As shown in Fig. 3, the fluorescence intensities decreased continuously and with a faint blue shift with the addition of increasing concentrations of Cu^{2+} to the peptide probe. The decrease in fluorescence intensity can be explained in terms of effective electron transfer from the excited dansyl fluorophore to the complexed copper cation.[15,53,54] Upon the addition of

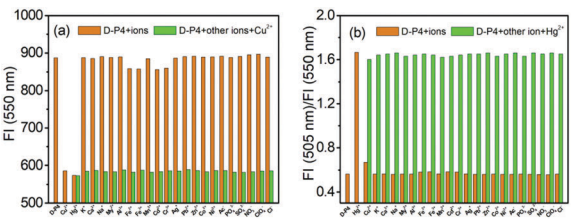

Fig. 2 Fluorescence response of DP-4 (20 μM) in the presence of 17 metal ions and 6 anions (1 equiv.) in 10 mM HEPES buffer at pH 7.1. The red bars represent the addition of these ions (20 μM) to the DP-4 solution. The green bars represent the subsequent addition of 20 μM Cu^{2+} (a) and Hg^{2+} (b) to the above solutions (λ_{ex} = 330 nm).

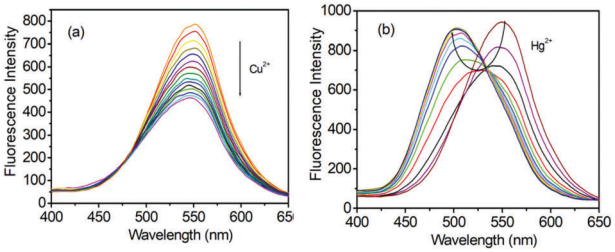

Fig. 3 Fluorescence emission spectra of D-P4 (20.0 μM) excited at 330 nm with the addition of increasing concentrations of Cu^{2+} (0–22.0 μM) (a) and Hg^{2+} (0–6.7 μM) (b) in 10 mM HEPES buffer at pH 7.1.

increasing concentrations of Hg^{2+}, the fluorescence intensities at 550 nm decreased and the intensities at 505 nm increased. Also, a 45 nm blue shift from 550 to 505 nm for the maximum fluorescence peak was observed, which indicates that D-P4 is a ratiometric probe for Hg^{2+} ions in HEPES buffer. In this titration curve, 1/3 equiv. Hg^{2+} was sufficient for saturation of the 45 nm blue shift, and a 3.2-fold ratiometric (FI_{550}/FI_{505}) change occurred after the addition of Hg^{2+}.

The excitation wavelength at 330 nm was employed for monitoring the dansyl fluorophore emission and 295 nm was employed for monitoring both the Trp and dansyl fluorophore emissions. While exciting at 295 nm, the fluorescence intensity of D-P4 at 355 nm and 550 nm decreased in the presence of Cu^{2+}, and the addition of Hg^{2+} caused the fluorescence intensity of D-P4 at 355 nm to decrease. However, the intensity at 550 nm increased and a 45 nm blue shift was observed (Fig. S1, ESI†). When Hg^{2+} interacts with amino acid residues of D-P4, the distance between the dansyl fluorophore (acceptor) and Trp residue (donor) is shortened, which may result in the folding of D-P4. This result indicates that the mechanism of the interaction between Hg^{2+} and D-P4 is the fluorescent resonance energy transfer (FRET) effect.

With the addition of increasing concentrations of Cu^{2+}, the fluorescence intensities at 355 nm and 550 nm gradually decreased. For the titration curve of Hg^{2+}, the maximum emission intensity of the dansyl fluorophore (550 nm) decreased and then increased, which was accompanied with a 45 nm blue shift (Fig. S2, ESI†).

Several chemosensors for monitoring Cu^{2+} and Hg^{2+} have been reported.[15–35,55–59] However, only a few sensors can selectively detect Cu^{2+} and Hg^{2+} *via* different channels. Lee *et al.*[15] reported a peptide-based sensor for the selective detection of Ag^{+}, Cu^{2+} and Hg^{2+} *via* different response types. In their peptide-based probe, two fluorophores, dansyl and Trp, were conjugated as an acceptor and donor for FRET, respectively.

Effects of pH on the detection for Cu^{2+} and Hg^{2+}

The influence of pH on the detection of D-P4 for Cu^{2+} and Hg^{2+} ions is shown in Fig. 4. At pH values lower than 5.0, D-P4 showed a very weak fluorescence intensity at 550 nm regardless of the absence and presence of Cu^{2+} and Hg^{2+}, which was attributed to the protonation of the imidazole ring of His and the electron-donating dimethyl amino group (pK_a = 4) of the

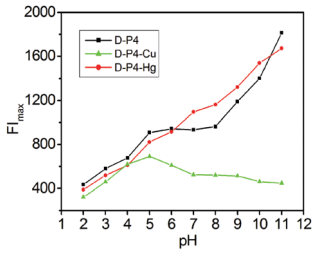

Fig. 4 Fluorescence intensity of D-P4 (20.0 μM) in the absence and presence of Cu^{2+} (1 equiv.) and Hg^{2+} (1/3 equiv.) ions at different pH values.

dansyl fluorophore at acidic pH.[37] However, at pH > 5.0, the fluorescence intensity of D-P4-Cu decreased and the fluorescence intensity of D-P4-Hg increased with an increase in pH, which was due to the deprotonation of the imidazole ring of His and sulfonamide group (pK_a = 10) of D-P4 in basic conditions.[15]

Binding stoichiometry and binding affinity

As shown in Fig. 5, the Job's plot exhibits a maximum at 0.5 mole fraction of Cu^{2+}, which indicates that a 1 : 1 complex was formed between D-P4 and Cu^{2+} in 10 mM HEPES buffer solution. In the case of Hg^{2+} monitoring, the Job's plot exhibited the maximum at a mole fraction of 0.25, indicating that D-P4 formed a 3 : 1 complex with Hg^{2+}.

According to the fluorescence titration curve (Fig. 3), the binding constants were calculated using the modified Benesi–Hildebrand equation. The binding constants K of D-P4 with Cu^{2+} and Hg^{2+} were calculated to be 8.82 × 10^4 M^{-1} and 2.87 × 10^5 $M^{-1/3}$, respectively (Fig. S3, ESI†).

Detection limit of D-P4 for Cu^{2+} and Hg^{2+}

The limits of detection of D-P4 for Cu^{2+} and Hg^{2+} were calculated using the good linear relationship of the fluorescence intensity at 550 nm with concentration of Cu^{2+} and Hg^{2+} ions (Fig. 6). According to the equation LOD = 3σ/m, the detection limits of DP-4 were 105.0 nM for Cu^{2+} and 37.0 nM for Hg^{2+}. This result indicates that the detection limits for Cu^{2+} is much lower than the standard EPA value for drinking water maximum contaminant levels.

Application for the detection of river water samples

The standard and measurement curves were obtained by standard addition of Cu^{2+} and Hg^{2+} to sample solutions. The results are summarized in Table 2a and b, and show that this fluorescent peptide probe exhibits a good recovery of 95.9.0% for Cu^{2+} in the range from 3 to 12 μM and 93.2% for Hg^{2+} in the range from 0.2 to 1.0 μM for monitoring Hg^{2+} and Cu^{2+} ions in river water. Therefore, these results indicate that this peptide probe can be used to monitor Cu^{2+} and Hg^{2+} ions in river water and has potential applications in the environmental field.

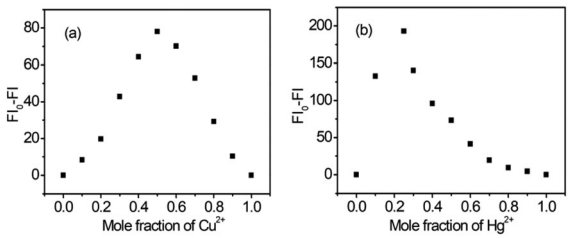

Fig. 5 Job's plots for D-P4 with Cu^{2+} (a) and Hg^{2+} (b) in 10 mM HEPES buffer at pH 7.1 (FI = FI$_{max}$).

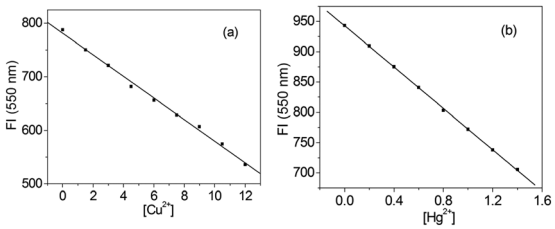

Fig. 6 Linear relationship of fluorescence intensity at 550 nm with concentration of Cu^{2+} (a) and Hg^{2+} (b) in 10 mM HEPES buffer at pH 7.1.

Table 2 (a) Determination of Hg^{2+} in river samples. (b) Determination of Cu^{2+} in river samples

(a)

Water sample	Hg^{2+} added (μM)	Hg^{2+} found (μM)	Recovery (%)
1	3.0	2.94	98.0
2	6.0	5.95	99.1
3	9.0	8.55	95.0
4	12.0	10.92	91.3

(b)

Water sample	Cu^{2+} added (μM)	Cu^{2+} found (μM)	Recovery (%)
1	0.2	0.18	90.1
2	0.4	0.35	87.5
3	0.6	0.58	96.7
4	0.8	0.75	93.8
5	1.0	0.98	98.0

UV/Vis and CD spectra of the D-P4-Cu^{2+}/Hg^{2+} systems

The interactions of D-P4 with Cu^{2+} and Hg^{2+} were investigated *via* UV/Vis absorption spectroscopy. The absorption spectrum of D-P4 shows four absorption bands at 220 nm, 250 nm, 280 nm, and 330 nm (Fig. S4, ESI†). Upon the addition of Cu^{2+}, the peak intensity at 220 nm decreased, but the peak intensities at 250 nm, 280 nm, and 330 nm increased. In contrast, in the absorption spectrum of D-P4 with the addition of Hg^{2+}, the absorption bands at 250 nm and 280 nm disappeared, while the absorption band at 330 nm exhibited a red shift. From the absorption spectra changes, we can infer that D-P4 may chelate with Cu^{2+} and Hg^{2+} *via* the sulfonamide group of the dansyl fluorophore and side chain group of the amino acid residues.

Circular dichroism (CD) spectroscopy is highly sensitive to structural changes in biomolecules. Fig. 7 illustrates the CD spectra of D-P4 in the absence and presence of Cu^{2+} and Hg^{2+} in 10 mM HEPES buffer. The CD spectrum of D-P4 consists of a positive band at 220 nm and a negative band at 250 nm. Upon the addition of Cu^{2+} and Hg^{2+}, the intensities of the 250 nm band decreased significantly and the intensity of the band at 220 nm changed from positive to negative. The degree of

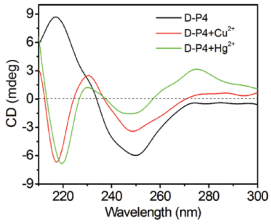

Fig. 7 CD spectra of D-P4 (100.0 μM) in the absence and presence of Cu^{2+} (0.5 equiv.) and Hg^{2+} (0.2 equiv.) in 10 mM HEPES buffer at pH 7.1.

change at 220 nm for Hg^{2+} was more than that for Cu^{2+}. Moreover, a positive band at 275 nm appeared after the addition of Hg^{2+}. Hence, we infer the formation of D-P4-Cu and D-P4-Hg complex systems from the conformational changes in the peptide probe.

Regeneration of the D-P4-Hg system

The regeneration of probes has always been important for the design of chemosensors. According to the hard and soft acid-base (HSAB) theory, thiol-containing Cys is regarded as an effective ligand for Hg^{2+} ions. Therefore, we chose Cys as a chelating agent for Hg^{2+}. The fluorescence emission spectrum of D-P4 was recovered perfectly when Cys was added to the D-P4-Hg system solution (Fig. S5a, ESI†). In addition, Cys did not influence the emission intensity of D-P4 (Fig. S5b, ESI†). When Hg^{2+} was added to the D-P4 solution containing Cys, the emission spectrum of D-P4 remained unchanged. In addition, the detection of Cu^{2+} using D-P4 was not affected. Therefore, Cys can be used to mask the interference of Hg^{2+} when selectively monitoring Cu^{2+}.

The addition of Cys restored the fluorescence emission peak of D-P4 because the thiol-containing Cys can remove Hg^{2+} from the D-P4-Hg system and release D-P4 (Fig. S4a, ESI†). Five detection cycles demonstrate that this probe is suitable for repeated use without considerable influence on the detection of Hg^{2+} (Fig. 8). Moreover, the UV/Vis and CD spectra also show that they can be well-restored when Cys was added to the D-P4-Hg system solution (Fig. S6 and S7, ESI,† respectively).

Detection of biothiols using the D-P4-Hg system

To evaluate the selectivity of D-P4-Hg for thiol-containing Cys, the emission spectrum of the D-P4-Hg system in the presence of 20 amino acids was recorded. Fig. 9a shows that the D-P4-Hg system exhibits exclusive selectivity for Cys *via* the restoration of fluorescence intensity and the maximum emission peak,

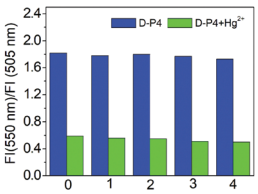

Fig. 8 Five detection cycles using the fluorescent peptide probe (D-P4 20.0 μM), Hg^{2+} (1/3 equiv.), and Cys (1/3 equiv.).

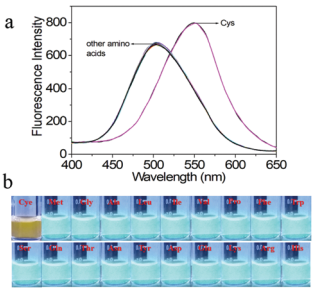

Fig. 9 (a) Fluorescence spectra of DP-4-Hg excited at 330 nm in the presence of 20 amino acids (10.0 μM) in 10 mM HEPES buffer at pH 7.1. (b) Emission color changes in the systems excited by a 365 nm UV lamp.

but it has no fluorescent response to the other 19 amino acids. Therefore, the D-P4-Hg system can selectively detect Cys, as indicated by the regeneration of the fluorescent peak without interference from 19 other amino acids. Fig. 9b shows the visible fluorescent color change of the D-P4-Hg system solution in the presence of Cys and 19 other amino acids under a 365 nm UV lamp. The D-P4-Hg system solution itself is a bright green color, but it was restored from a green color to a yellow color when Cys was added to this solution. However, the D-P4-Hg systems containing the 19 other amino acids still displayed a bright green color.

The D-P4 system can selectively distinguish Cys from other amino acids. Thus, it was important to further investigate whether the D-P4 system can distinguish thiol-containing Cys, Hcy and GSH from one another because the structures and reactivity of these biothiols are similar. As shown in Fig. 10, the addition of Cys, Hcy, and GSH restored the fluorescence peak of the D-P4-Hg system to the state of D-P4. This result shows that the D-P4-Hg system can effectively monitor these biothiols.

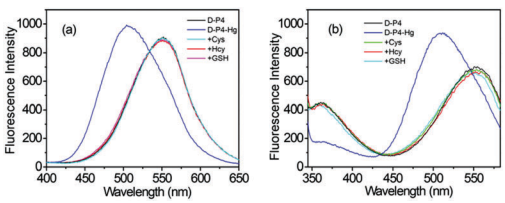

Fig. 10 Fluorescence spectra of DP-4 (20 μM) and D-P4-Hg(7.0 μM) in the presence of Cys, Hcy and GSH (10.0 μM) in 10 mM HEPES buffer at pH 7.1. (a) λ_{ex} = 330 nm and (b) λ_{ex} = 295 nm.

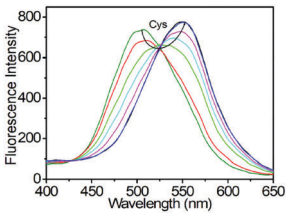

Fig. 11 Fluorescence emission spectra of D-P4-Hg (6.7 μM) with the addition of increasing concentrations of Cys (0–7.5 μM) in 10 mM HEPES buffer at pH 7.1 (λ_{ex} = 330 nm).

Table 3 Various spectral sensing systems for the determination of Cys

Method	System	Detection limit	Ref.
Fluorescence	Curcumin and Hg^{2+} system	1.0 μM	60
Fluorescence	Naphthol AS-based sensor	500.0 nM	61
Fluorescence	Diketopyrrolopyrrole-based chemodosimeter	5.0 μM	62
Fluorescence	HMBQ-Nap 1	29.0 nM	63
Fluorescence	Quinazoline platform	350.0 nM	64
Fluorescence	π-Conjugated triarylboron luminogen	180.0 nM	65
Fluorescence	D-P4-Hg system	82.0 nM	This study
Fluorescence	Acridine orange	110.0 nM	46
Fluorescence	Hg^{2+}-Sensor complex	5.2 μM	66
Fluorescence	A benzothiazole derivative	84.0 nM	67
Absorption	Hg^{2+}-Sensor complex	100.0 nM	9
Absorption	PBI-Hg^{2+}	91.0 nM	68

To further determine the LOD of D-P4-Hg for biothiols, the fluorescence titration of cysteine was conducted. As shown in Fig. 11, the emission intensity returned to the initial state of D-P4 after the addition of 1 equiv. Cys to the DP-4-Hg system solution. According to the good linear relationship between the fluorescent intensity at 505 nm and the concentration of Cys, the LOD of the system for monitoring Cys was calculated to be 82.0 nM (Fig. S8, ESI†). From Table 3, it can be seen that the D-P4-Hg system has lower detection limit for Cys than that in previous reports.

Conclusions

In conclusion, a new multi-functional peptide-based fluorescent probe was synthesized for the detection of Cu^{2+} and Hg^{2+}. D-P4 showed highly selective and sensitive fluorescence response to Cu^{2+} *via* a turn-off response and Hg^{2+} *via* a ratiometric response, which rendered low detection limits. This peptide-based fluorescent probe exhibited good practicality for river water samples without performing tedious sample pretreatments. In addition, D-P4 was used for the cyclic detection of Hg^{2+} under the treatment of cysteine. Furthermore, the D-P4-Hg system was also successfully used to monitor biothiols. Significantly, this peptide-based probe exhibits numerous advantages including easy synthesis, good water solubility, excellent sensitivity and selectivity, fast response and good reversibility. Therefore, we anticipate that this probe can promote the development of peptide-based sensor and has potential practical application in the environment.

Conflicts of interest

There are no conflicts to declare.

Acknowledgements

This study was supported by the Scientific Research Foundation of Liaocheng University, China (318011513), and the National Natural Science Foundation of China (21142003, 20471025), the Natural Science Foundation of Shandong Province of China (ZR2016HB73).

References

1 B. Bansod, T. Kumar, R. Thakur, S. Rana and I. Singh, *Biosens. Bioelectron.*, 2017, **94**, 443–455.
2 V. Karri, V. Kumar, D. Ramos, E. Oliveira and M. Schuhmacher, *Biol. Trace Elem. Res.*, 2017, **4**, 1–14.
3 M. Jahiruddin, Y. Xie, A. Ozaki, M. R. Islam, T. V. Nguyen and K. Kurosawa, *Aust. J. Crop Sci.*, 2017, **11**, 806–812.
4 H. N. Kim, W. X. Ren, J. S. Kim and J. Yoon, *Chem. Soc. Rev.*, 2012, **41**, 3210–3244.
5 W. F. Fitzgerald, C. H. Lamborg and C. R. Hammerschmidt, *Chem. Rev.*, 2007, **107**, 641–662.
6 O. Malm, *Environ. Res., Sect. A*, 1998, **77**, 73–78.
7 H. H. Harris, I. J. Pickering and G. N. George, *Science*, 2003, **301**, 1203.
8 M. J. Scoullos, G. H. Vonkeman, I. Thornton and Z. Makuch, *Environ. Sci. Policy*, 2001, **45**, 367–387.
9 J. M. Jung, C. Kim and R. G. Harrison, *Sens. Actuators, B*, 2018, **255**, 2756–2763.
10 J. Kumar, P. K. Bhattacharyya and D. K. Das, *Spectrochim. Acta, Part A*, 2015, **138**, 99–104.
11 S. Cao, Q. Jin, L. Geng, L. Mu and S. Dong, *New J. Chem.*, 2016, **40**, 6264–6269.
12 D. Wu, A. C. Sedgwick, T. Gunnlaugsson, E. U. Akkaya, J. Yoon and T. D. James, *Chem. Soc. Rev.*, 2017, **46**, 7105–7123.
13 Z. Shekari, H. Younesi, A. Heydari, M. Tajbakhsh, M. J. Chaichi, A. Shahbazi and D. Saberi, *Chemosensors*, 2017, **5**, 26.
14 A. L. Suherman, S. Kuss, E. Tanner, N. P. Young and R. G. Compton, *Analyst*, 2018, **143**, 2035–2041.
15 L. N. Neupane, P. Thirupathi, S. Jang, M. J. Jang, J. H. Kim and K. H. Lee, *Talanta*, 2011, **85**, 1566–1574.
16 P. Wang, L. Liu, P. Zhou, W. Wu, J. Wu, W. Liu and Y. Tang, *Biosens. Bioelectron.*, 2015, **72**, 80–86.
17 B. R. White and J. A. Holcombe, *Talanta*, 2007, **71**, 2015–2020.
18 J. Liu and Y. Lu, *J. Am. Chem. Soc.*, 2007, **129**, 9838–9839.
19 S. H. Kim, J. S. Kim, S. M. Park and S. K. Chang, *Org. Lett.*, 2006, **8**, 371–374.
20 T. Sun, Q. Niu, T. Li, Z. Guo and H. Liu, *Spectrochim. Acta, Part A*, 2017, **188**, 411–417.

21 J. H. Ye, J. Xu, H. Chen, Y. Bai, W. Zhang and W. He, *Tetrahedron Lett.*, 2014, **55**, 6269–6273.
22 J. X. Su, X. T. Wang, J. Chang, G. Y. Wu, H. M. Wang, H. Yao, Q. Lin, Y. M. Zhang and T. B. Wei, *Spectrochim. Acta, Part A*, 2017, **182**, 67–72.
23 I. J. Chang, M. G. Choi, A. J. Yong, H. L. Sang and S. K. Chang, *Tetrahedron Lett.*, 2017, **58**, 474–477.
24 C. Zou, L. Gao and T. Liu, *J. Inclusion Phenom. Macrocyclic Chem.*, 2014, **80**, 383–390.
25 C. R. Lohani, L. N. Neupane, J. M. Kim and K. H. Lee, *Sens. Actuators, B*, 2012, **161**, 1088–1096.
26 B. R. White, H. M. Liljestrand and J. A. Holcombe, *Analyst*, 2008, **133**, 65–70.
27 B. P. Joshi, J. Park, W. I. Lee and K. H. Lee, *Talanta*, 2009, **78**, 903–909.
28 J. Park, B. In and K. H. Lee, *RSC Adv.*, 2015, **5**, 56356–56361.
29 D. H. Kim, J. Seong, H. Lee and K. H. Lee, *Sens. Actuators, B*, 2014, **196**, 421–428.
30 N. Wanichacheva, K. Setthakarn, N. Prapawattanapol, O. Hanmeng, V. S. Lee and K. Grudpan, *J. Lumin.*, 2012, **132**, 35–40.
31 Y. W. Sie, C. L. Li, C. F. Wan, H. Yan and A. T. Wu, *J. Photochem. Photobiol., A*, 2018, **353**, 19–25.
32 J. Chen, Y. Li, W. Zhong, H. Wang, P. Zhang and J. Jiang, *Anal. Methods*, 2016, **8**, 1964–1967.
33 F. Y. Wu, Y. Q. Zhao, Z. J. Ji and Y. M. Wu, *J. Lumin.*, 2007, **17**, 460–465.
34 J. Wu, L. Li, D. Zhu, P. He, Y. Fang and G. Cheng, *Anal. Chim. Acta*, 2011, **694**, 115–119.
35 J. Yang, H. Rong, P. Shao, Y. Tao, J. Dang, P. Wang, Y. Ge, J. Wu and D. Liu, *J. Mater. Chem. B*, 2016, **4**, 6065–6073.
36 Y. Li, L. Li, X. Pu, G. Ma, E. Wang, J. Kong, Z. Liu and Y. Liu, *Bioorg. Med. Chem. Lett.*, 2012, **22**, 4014–4017.
37 B. In, G. W. Hwang and K. H. Lee, *Med. Chem. Lett.*, 2016, **26**, 4477–4482.
38 Q. Liu, J. Wang and B. J. Boyd, *Talanta*, 2015, **136**, 114–127.
39 I. Dokmanić, M. Sikić and S. Tomić, *Acta Crystallogr., Sect. D: Biol. Crystallogr.*, 2008, **64**, 257–263.
40 Q. Wang, J. Cui, G. Li, J. Zhang, F. Huang and Q. Wei, *Polymers*, 2014, **6**, 2357–2370.
41 E. Pazos, O. Vázquez, J. L. Mascareñas and M. E. Vázquez, *Chem. Soc. Rev.*, 2009, **38**, 3348–3359.
42 C. Luo, Q. Zhou, B. Zhang and X. Wang, *New J. Chem.*, 2011, **35**, 45–48.
43 Q. Lin, Y. Huang, J. Fan, R. Wang and N. Fu, *Talanta*, 2013, **114**, 66–72.
44 N. Haugaard, *Ann. N. Y. Acad. Sci.*, 2010, **899**, 148–158.
45 I. A. Alov, M. E. Aspiz and N. A. Palkina, *Zh. Obshch. Biol.*, 1969, **30**, 452.
46 Y. Tang, L. Jin and B. Yin, *Anal. Chim. Acta*, 2017, **993**, 87–95.
47 S. Shahrokhian, *Anal. Chem.*, 2001, **73**, 5972–5978.
48 M. T. Heafield, S. Fearn, G. B. Steventon, R. H. Waring, A. C. Williams and S. G. Sturman, *Neurosci. Lett.*, 1990, **110**, 216–220.
49 B. Hooshmand, T. Polvikoski, M. Kivipelto, M. Tanskanen, L. Myllykangas, T. Erkinjuntti, M. Mäkelä, M. Oinas, A. Paetau, P. Scheltens, E. C. van Straaten, R. Sulkava and A. Solomon, *Brain*, 2013, **136**, 2707–2716.
50 S. Sarkar, S. Roy, R. N. Saha and S. S. Panja, *J. Fluoresc.*, 2018, **28**, 427–437.
51 S. Das, A. Sahana, A. Banerjee, S. Lohar, D. A. Safin, M. G. Babashkina, M. Bolte, Y. Garcia, I. Hauli, S. K. Mukhopadhyay and D. Das, *Dalton Trans.*, 2013, **42**, 4757–4763.
52 J. J. Pinto, C. Moreno and M. G. Vargas, *Talanta*, 2004, **64**, 562–565.
53 R. A. Bissell, A. P. de Silva, H. Q. N. Gunarantne, P. L. M. Lynch, G. E. M. Maguire, C. P. McCoy and K. R. A. S. Sandanayake, *Top. Curr. Chem.*, 1993, **168**, 223.
54 H. Masuhara, H. Shioyama, T. Saito, K. Hamada, S. Yasoshima and N. Mataga, *J. Phys. Chem.*, 1984, **88**, 5868–5873.
55 G. Li, F. Tao, Q. Liu, L. Wang, Z. Wei, F. Zhu, W. Chen, H. Sun and Y. Zhou, *New J. Chem.*, 2016, **40**, 4513–4518.
56 Q. Yue, T. Shen, J. Wang, L. Wang, S. Xu, H. Li and J. Liu, *Chem. Commun.*, 2013, **49**, 1750–1752.
57 T. Shen, Q. Yue, X. Jiang, L. Wang, S. Xu, H. Li, X. Gu, S. Zhang and J. Liu, *Talanta*, 2013, **117**, 81–86.
58 L. J. Wang, L. P. Jia, R. N. Ma, W. L. Jia and H. S. Wang, *Anal. Methods*, 2017, **9**, 5121–5126.
59 Y. Zhang, R. Li, Q. Xue, H. Li and J. Liu, *Microchim. Acta*, 2015, **182**, 1677–1683.
60 F. Geng, Y. Wang, P. Qu, Y. Zhang, H. Dong and M. Xu, *Anal. Methods*, 2013, **5**, 3965–3969.
61 W. Ma, M. Wang, D. Yin and X. Zhang, *Sens. Actuators, B*, 2017, **248**, 332–337.
62 W. Qu, L. Yang, Y. Hang, X. Zhang, Y. Qu and J. Hua, *Sens. Actuators, B*, 2015, **211**, 275–282.
63 R. Nawimanage, B. Prasai, S. U. Hettiarachchi and R. L. Mccarley, *Anal. Chem.*, 2014, **86**, 12266–12271.
64 T. Anand, G. Sivaraman and D. Chellappa, *Spectrochim. Acta, Part A*, 2014, **123**, 18–24.
65 X. Guo, X. Zhang, S. Wang, S. Li, R. Hu and Y. Li, *Anal. Chim. Acta*, 2015, **869**, 81–88.
66 W. C. Ye, J. J. Lee, G. R. You and C. Kim, *RSC Adv.*, 2015, **5**, 38308–38315.
67 S. Feng, X. Li, Q. Ma, B. Liang and Z. Ma, *Anal. Methods*, 2016, **8**, 6832–6839.
68 H. P. Fang, M. Shellaiah, A. Singh, Y. H. Wu and H. C. Lin, *Sens. Actuators, B*, 2014, **194**, 229–237.